NATIONAL AERONAUTICS AND SPACE ADMINISTRATION

MSC INTERNAL NOTE NO. 69-FM-149

June 2, 1969

AN EMPIRICAL TECHNIQUE FOR COMPUTING NAVIGATION COVARIANCE MATRICES AND THE APPLICATION OF THE TECHNIQUE TO POST APOLLO 8 LUNAR ORBIT MISSION PLANNING

Mathematical Physics Branch

MISSION PLANNING AND ANALYSIS DIVISION

MANNED SPACECRAFT CENTER

USTON, TEXAS

MSC INTERNAL NOTE NO. 69-FM-149

PROJECT APOLLO

AN EMPIRICAL TECHNIQUE FOR COMPUTING NAVIGATION COVARIANCE MATRICES AND THE APPLICATION OF THE TECHNIQUE TO POST APOLLO 8 LUNAR ORBIT MISSION PLANNING

By John Bruce Williamson
Mathematical Physics Branch

June 2, 1969

MISSION PLANNING AND ANALYSIS DIVISION
NATIONAL AERONAUTICS AND SPACE ADMINISTRATION
MANNED SPACECRAFT CENTER
HOUSTON, TEXAS

Approved: _____
James C. McPherson, Chief
Mathematical Physics Branch

Approved: _____
John P. Mayer, Chief
Mission Planning and Analysis Division

FIGURES

AN EMPIRICAL TECHNIQUE FOR COMPUTING NAVIGATION COVARIANCE MATRICES AND THE APPLICATION OF THE TECHNIQUE TO POST APOLLO 8 LUNAR ORBIT MISSION PLANNING

By John Bruce Williamson

SUMMARY

An empirical technique used to calculate navigation covariance matrices is presented which is based on actual postflight tracking data processing from the Apollo 8 mission and the Langley Lunar Orbiter III. Postflight analyses of the Apollo 8 mission and Lunar Orbiter III revealed that the lunar gravitational potential function was not known as well as had been assumed before these missions. There is not sufficient information available at this writing to provide a satisfactory statistical description of the uncertainty in the model. This technique requires as input empirical errors in certain orbital parameters determined from postflight analysis. A numerical description (covariance matrix) of the anticipated navigation accuracies in lunar orbit is produced by the use of this technique. The technique is reasonably independent of the potential model which is used to process tracking data, although different values for the input parameters must be determined for each model.

This technique has been applied to Apollo Missions F and G and has been found to model secular growth in down-track position errors satisfactorily. The technique is limited in its capability to model the smaller growth rates expected in radial position errors, and it does not model oscillatory errors in the radial and down-track components of position and velocity as well as might be desired. A conservative estimate of the navigation accuracy is obtained when the oscillatory behavior is modeled as an independent secular error the magnitude of which is the amplitude of the oscillation. By careful application, this technique can be used to convert the results of postflight studies into the numerical input required for other mission planning tools (e.g., dispersion analysis programs).

INTRODUCTION

Analysis of tracking from the Langley Lunar Orbiter program showed an unusual Doppler data residual pattern. Therefore, navigation of a spacecraft in lunar orbit with a perilune altitude of less than a few hundred miles could be inaccurate. Experts generally agree that this navigation problem is the result of an inaccurate lunar gravitational potential function. In other words, a significant amount of uneven mass distribution is present near the lunar surface. Analytic procedures for estimation of navigation accuracies require that all sources of error be precisely defined and that the probability distribution functions of the parameters be known. Studies are now being conducted to find the best lunar gravitational potential model for spacecraft navigation and the appropriate values to be assigned to the coefficients in the model. The probability distributions for the model are unknown at present. When a satisfactory model is implemented, the parameters of its probability distribution will be determined by processing tracking data from a number of different spacecraft. The primary effect of this problem is on processing earth-based radar data.

ABBREVIATIONS AND SYMBOLS

a	semimajor axis of spacecraft orbit
MSC	Manned Spacecraft Center
MSFN	Manned Space Flight Network
n	number of revolutions over which the covariance matrix is to be valid
PTEAP	Perturbed Trajectory Error Analysis Program
LOI-1	first lunar orbit insertion maneuver
LOI-2	circularization maneuver
R	spacecraft position vector
RSS	root sum square
RTCC	Real-Time Computer Complex
r	radius to spacecraft, $r = \|R\|$

s	speed of spacecraft, $s = \|V\|$
u v w coordinate system	spacecraft local orbit plane coordinate system defined inertially at a given time by the unit vectors $i = R/r$, $j = (RxV)xR/\|(RxV)xR\|$, $k = RxV/\|RxV\|$
V	spacecraft velocity vector
u_g, v_g, θ_g, γ_g	growth rates per revolution of the errors in local radius, down-track radius, orbital plane wedge anlge, and flight-path angle
u_o, v_o, θ_o, γ_o	initial errors at the MSFN tracking epoch in local radius, down-track position, orbit plane wedge angle, and flight-path angle
$\Delta\dot{u}$, Δv, etc.	incremental change in $\dot{u}$, v, etc.
μ	gravitational constant of central body
ρ_{ij}	the correlation coefficient between the i^{th} and j^{th} parameters
σ_u, σ_v, σ_w, $\sigma_{\dot{u}}$, $\sigma_{\dot{v}}$, $\sigma_{\dot{w}}$	standard deviations in the components of the spacecraft position and velocity vectors, expressed in the u v w coordinate system

$\sigma_{u\dot{v}}$	covariance between radial position and down-track velocity
$\sigma_{v\dot{u}}$	covariance between down-track position and radial velocity
σ_{γ}	standard deviation in flight-path angle
σ_{τ}	standard deviation in orbital period
τ	period of spacecraft orbit

PROCEDURE

The Mathematical Physics Branch of MSC has suspended the use of ordinary analytic tools for analyzing lunar orbit navigation based on the MSFN S-band radar stations. Instead, an interim technique has been devised which empirically models the trajectory effects observed in postflight processing of Lunar Orbiter III and Apollo 8 tracking data. This technique deals with trajectory parameters only and does not attempt to define the lunar potential model. Postflight data processing provides the inputs to the technique as local errors and propagation effects observed with a particular lunar potential model. The resultant navigation accuracies are checked by propagating them with the standard analytic tools and by comparing these results with the postflight results. This assures that the application of the results (e.g., dispersion analysis) using existing analytic tools will approximate the actual behavor of the spacecraft as observed in real time, to within the accuracy provided by the calibration with postflight results.

ANALYSIS

The current technique used to generate covariance matrices for vehicles in lunar orbit is based on the assumption that the navigation errors consist of independent local fit errors in four parameters and, independently, growth rates in these errors because of propagation. These parameters are as follows.

- u the local radius
- v the local down-track position
- θ the angle between the estimated and actual angular momentum vectors
- γ the local flight-path angle of the vehicle

All other errors in the state vector of the vehicle are derived from this set. In general, the growth rate θ_g in θ errors is so small that it is neglected for these studies.

The MSFN tracking epoch is assumed to be in the middle of a front-side pass at approximately 0° longitude. This choice is arbitrary, and was made because it resulted in a formulation for out-of-plane errors which is convenient for lunar landing and rendezvous studies. If the tracking epoch is chosen to be in the middle of the data arc for one pass, the following equations are assumed for cross-track position and velocity errors.

$$\sigma_w \simeq 0$$
$$\sigma_{\dot{w}} = s \sin(\theta_0) \qquad (1)$$

To account for some uncertainty in the longitude of the ascending node and argument of latitude at the fit epoch σ_w is customarily set equal to 1000 feet. This does not result in a significant change in θ_0.

The errors in radial position and flight-path angle must be constructed to include the error growth rate for a certain number of revolutions n. This construction is required because ordinary covariance propagation techniques do not model growths in these errors, which is one of the main restrictions on the technique.

$$\sigma_u^2 = (u_0)^2 + (n \times u_g)^2$$
$$\sigma_\gamma^2 = (\gamma_0)^2 + (n \times \gamma_g)^2 \qquad (2)$$

The growth rate in down-track position error is the most significant error growth, and this growth can be modeled with current propagation techniques. Therefore, the error in down-track position at the tracking epoch is simply

$$\sigma_v = v_0 \qquad (3)$$

The development of the equations for the radial and down-track velocity errors and their covariances with the radial and down-track position errors are included in the appendix. In summary, the equations are the following.

$$\sigma_{\dot{u}}^2 = \left(-\frac{s}{r}\right)^2 \sigma_v^2 + s^2 \sigma_\gamma^2 \qquad (4)$$

$$\sigma_{\dot{v}}^2 = \left(-\frac{s}{r}\right)^2 \sigma_u^2 + \left(\frac{v_g}{3\tau}\right)^2 \qquad (5)$$

$$\sigma_{u\dot{v}} = -\frac{s}{r} \sigma_u^2 \qquad (6)$$

$$\sigma_{v\dot{u}} = -\frac{s}{r} \sigma_v^2 \qquad (7)$$

All other correlation coefficients are zero.

The covariance matrix at the MSFN tracking epoch may be found by use of equation (1) (modified) and equations (2) through (7). Because this matrix is symmetric, the numbers in the lower triangular portion are replaced by their corresponding correlation coefficients, which convey more intuitive information than covariances. The equation for the correlation coefficient is

$$\rho_{ij} = \frac{\sigma_{ji}}{\sigma_i \sigma_j} \qquad (8)$$

The covariance matrix is always presented in the vehicle's local u v w coordinate system defined inertially at the time associated with the matrix.

RESULTS

The error models empirically determined from unpublished post-flight tracking data analyses of the Langley Lunar Orbiter III and Apollo 8 are presented in table I. The three cases were used to provide navigation accuracies for Mission F planning and dispersion analysis support. Case 1 represents the assumptions that one pass of MSFN data will be processed in the RTCC orbit determination program with a triaxial lunar gravitational potential model and that both RTCC and on-board state vector predictors will use the triaxial model. Case 2 represents the assumptions that one pass of MSFN data will be processed

with the Boeing R-2 lunar gravitational potential model (ref. 1) and that both ground and onboard state vector predictors will use the R-2 potential model. Case 3 is the same as case 2 except that data from two consecutive passes will be processed. The Perturbed Trajectory Error Analysis Program (PTEAP) (ref. 2) was used to predict the state vector uncertainties for the next two revolutions. The initial covariance matrices for these three cases are presented in table II. Plots of the predicted component and RSS position and velocity uncertainties for cases 1 through 3 are presented in figures 1, 2, and 3.

For comparison, postflight state vector comparisons from Apollo 8 that correspond to case 3 are presented in figure 4. A state vector was determined from the two-pass data arc in revolutions three and four by constraining the orbital plane to coincide with the orbital plane determined by a prediction of the pre-LOI-1 state vector through the confirmed LOI-1 and LOI-2 maneuvers. This vector was compared with the local one-pass unconstrained state vector solutions for revolutions four, five, and six. These comparisons are presented as differences in the components of the state vectors in the local u v w coordinate system. The view periods for this mission last from 40 minutes after the beginning of the revolution until 1 hour 50 minutes after the beginning of the revolution. Comparisons between error analysis and postflight results should be made only during the view period.

CONCLUSIONS

The results presented are not intended to be independent determinations of navigation accuracies for Apollo missions. Rather, the technique is presented by which insight from postflight tracking data analyses is transformed into numerical input for the various studies which are performed in planning an Apollo-type mission. The figures should be compared with the postflight analyses to verify the technique. This comparison has been made informally and indicates that the technique models cases 1 and 2 quite accurately. In case 3, postflight analyses have revealed undamped (i.e., growing in amplitude) oscillatory errors, especially in radial position and down-track velocity (fig. 4), which are not modeled by this technique. However, the technique does model the secular effects satisfactorily. A conservative estimation of the navigation accuracies is obtained if the oscillatory behavior is modeled as an independent secular error the magnitude of which is the amplitude of the oscillation. Case 3 is by far the most satisfactory from a navigation standpoint. The cross-track errors in case 3 are the same as in case 2 because the cross-track components of the state vector are determined by a one-pass data fit, and the two-pass fit is constrained to maintain these values. Recent unpublished

postflight analyses indicate that a better estimation of cross-track position and velocity during lunar orbit operations can be obtained by prediction of the pre-LOI-1 state vector through the confirmed maneuvers. This technique would be used with the one-pass technique as a monitoring tool. Hence, the error estimates described in this note should be conservative in cross-track position and velocity.

TABLE I.- ERROR MODELS

Parameter	Case I	Case II	Case III
u_0, ft	1000	1000	1000
v_0, ft	3000	3000	3000
θ_0, deg	0.1	0.1	0.1
γ_0, deg	.01	.01	.01
u_g ft/rev	1500	500	500
v_g, ft/rev	15 000	11 000	1500
θ_g, deg/rev	.005	.005	.005
γ_g, deg/rev	.005	.005	.005

TABLE II.- COVARIANCE MATRICES FOR LUNAR ORBIT

MANNED SPACE FLIGHT NETWORK (MSFN) TRACKING DATA

(a) Navigation covariance matrix for case 1, one-pass triaxial fit at MSFN tracking epoch[a]

$$\begin{bmatrix} 9.9999996 \times 10^6 & 0 & 0 & 0 & -8809.4843 & 0 \\ 0 & 9.0 \times 10^6 & 0 & -7928.5361 & 0 & 0 \\ 0 & 0 & 1.0 \times 10^6 & 0 & 0 & 0 \\ 0 & -.78466998 & 0 & 11.344084 & 0 & 0 \\ -.97036671 & 0 & 0 & 0 & 8.2429547 & 0 \\ 0 & 0 & 0 & 0 & 0 & 81 \end{bmatrix}$$

(b) Navigation covariance matrix for case 2, one-pass R-2 fit at MSFN tracking epoch[a]

$$\begin{bmatrix} 2.0 \times 10^6 & 0 & 0 & 0 & -1761.8969 & 0 \\ 0 & 9.0 \times 10^6 & 0 & -7928.5361 & 0 & 0 \\ 0 & 0 & 1.0 \times 10^6 & 0 & 0 & 0 \\ 0 & -.8945489 & 0 & 8.7284141 & 0 & 0 \\ -.92565272 & 0 & 0 & 0 & 1.8114854 & 0 \\ 0 & 0 & 0 & 0 & 0 & 88.063182 \end{bmatrix}$$

[a]Format for matrices in table II.

$$\begin{bmatrix} (\sigma_u)^2 & 0 & 0 & 0 & \sigma_{u\dot{v}} & 0 \\ 0 & (\sigma_v)^2 & 0 & \sigma_{v\dot{u}} & 0 & 0 \\ 0 & 0 & (\sigma_w)^2 & 0 & 0 & 0 \\ 0 & \rho_{v\dot{u}} & 0 & (\sigma_{\dot{u}})^2 & 0 & 0 \\ \rho_{u\dot{v}} & 0 & 0 & 0 & (\sigma_{\dot{v}})^2 & 0 \\ 0 & 0 & 0 & 0 & 0 & (\sigma_{\dot{w}})^2 \end{bmatrix}$$

TABLE II.- COVARIANCE MATRICES FOR LUNAR ORBIT

MANNED SPACE FLIGHT NETWORK (MSFN) TRACKING DATA - Continued

(c) Navigation covariance matrix for case 3, two-pass R-2 fit, at MSFN tracking epoch[a]

$$\begin{bmatrix} 2.0 \times 10^6 & 0 & 0 & 0 & -1761.897 & 0 \\ 0 & 9.0 \times 10^6 & 0 & -7928.536 & 0 & 0 \\ 0 & 0 & 1.0 \times 10^6 & 0 & 0 & 0 \\ 0 & -0.89455 & 0 & 8.728412 & 0 & 0 \\ -0.99845 & 0 & 0 & 0 & 1.556963 & 0 \\ 0 & 0 & 0 & 0 & 0 & 81.0 \end{bmatrix}$$

[a]Format for matrices in table II.

$$\begin{bmatrix} (\sigma_u)^2 & 0 & 0 & 0 & \sigma_{u\dot{v}} & 0 \\ 0 & (\sigma_v)^2 & 0 & \sigma_{v\dot{u}} & 0 & 0 \\ 0 & 0 & (\sigma_w)^2 & 0 & 0 & 0 \\ 0 & \rho_{v\dot{u}} & 0 & (\sigma_{\dot{u}})^2 & 0 & 0 \\ \rho_{u\dot{v}} & 0 & 0 & 0 & (\sigma_{\dot{v}})^2 & 0 \\ 0 & 0 & 0 & 0 & 0 & (\sigma_{\dot{w}})^2 \end{bmatrix}$$

TABLE II.- COVARIANCE MATRICES FOR LUNAR ORBIT

MANNED SPACE FLIGHT NETWORK (MSFN) TRACKING DATA - Concluded

(d) Summary

Case	RSS position uncertainty, ft	RSS velocity uncertainty, fps	σ_u, ft	σ_v, ft	σ_w, ft	$\sigma_{\dot{u}}$, fps	$\sigma_{\dot{v}}$, fps	$\sigma_{\dot{w}}$, fps
I	4472	10.03	3162	3000	1000	3.37	2.87	9.00
II	3464	9.93	1414	3000	1000	2.95	1.35	9.38
III	3464	9.55	1414	3000	1000	2.95	1.25	9.00

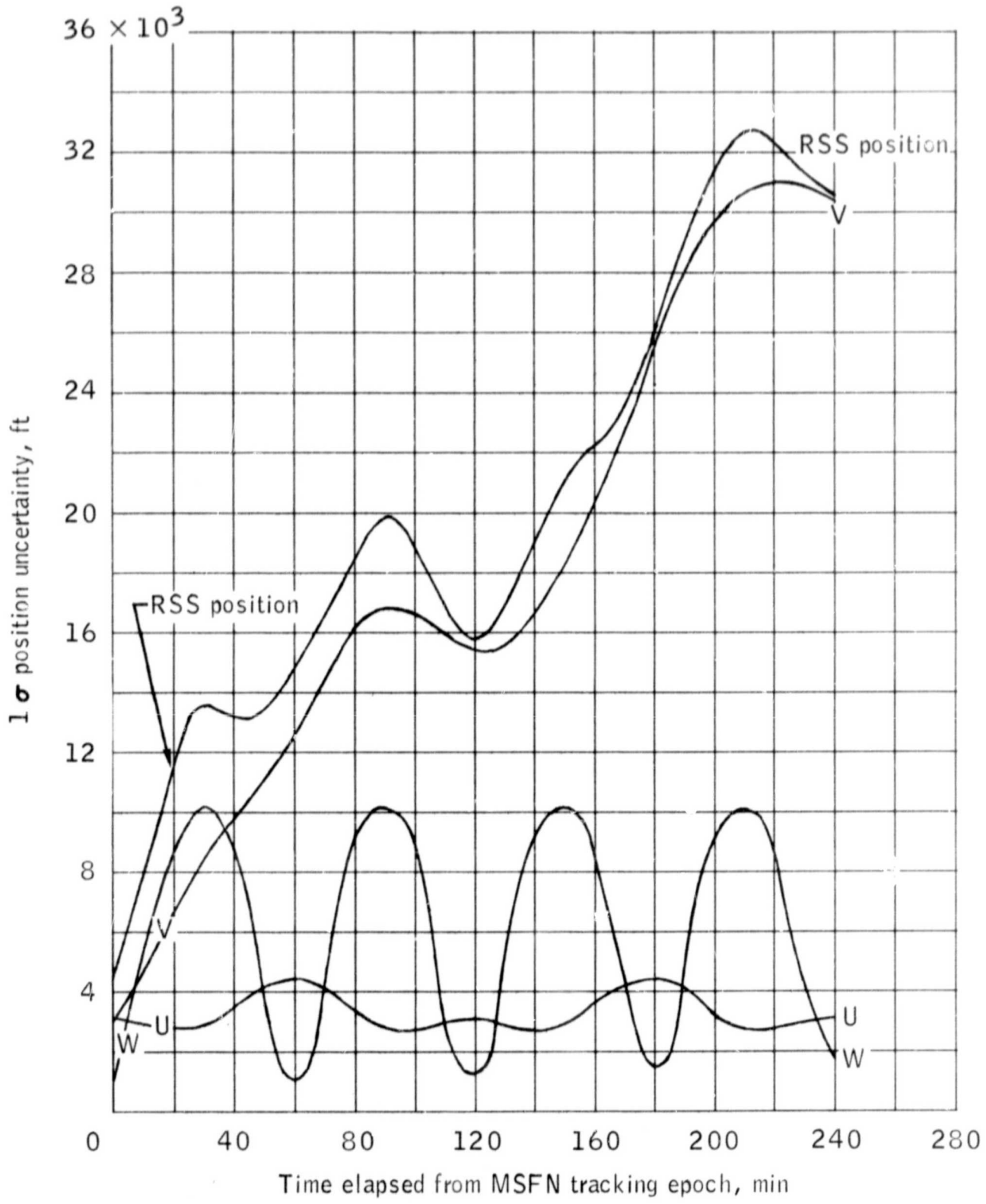

(a) One sigma position.

Figure 1.- One pass MSFN solution accuracies, triaxial lunar potential model.

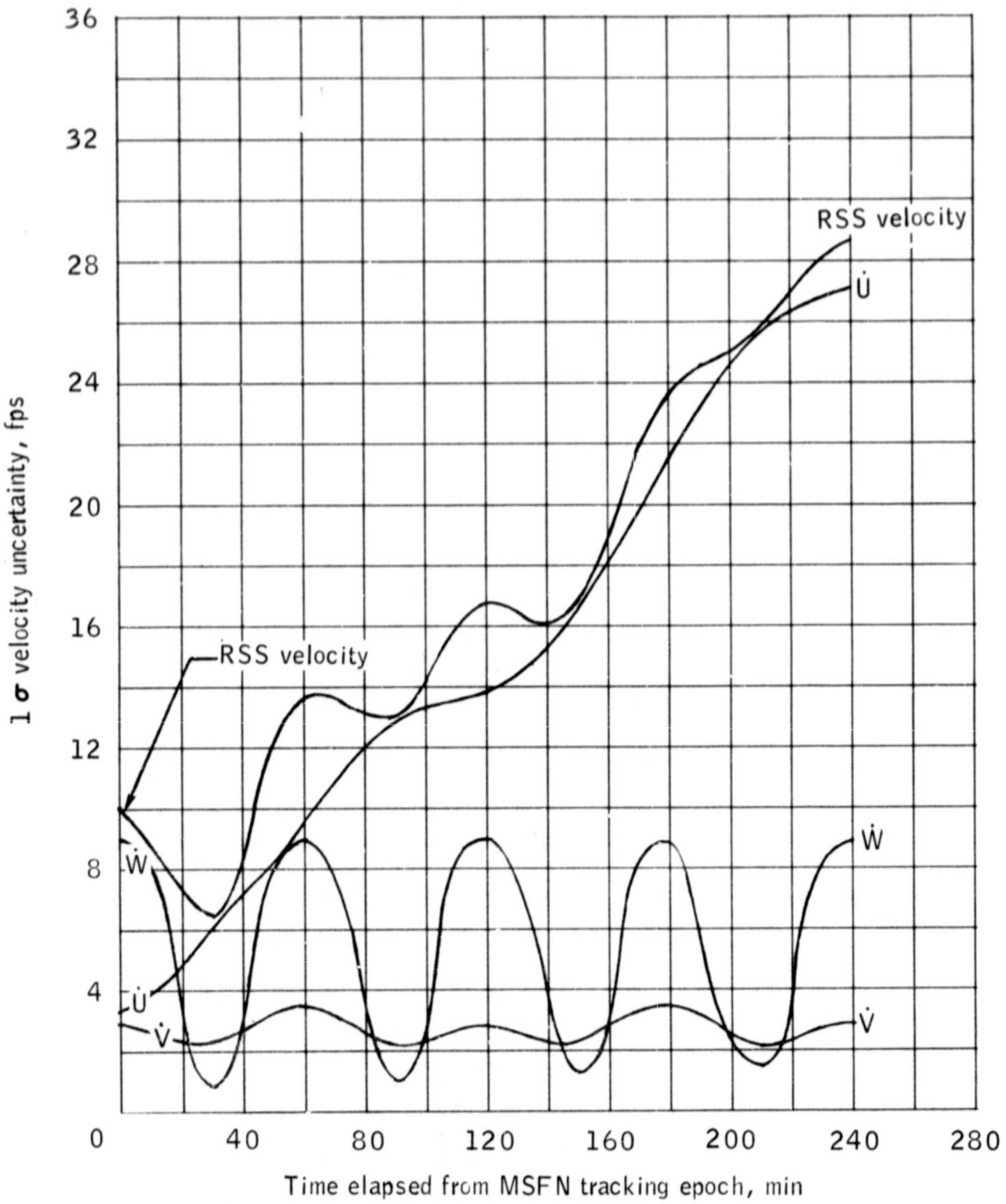

(b) One sigma velocity.

Figure 1.- Concluded.

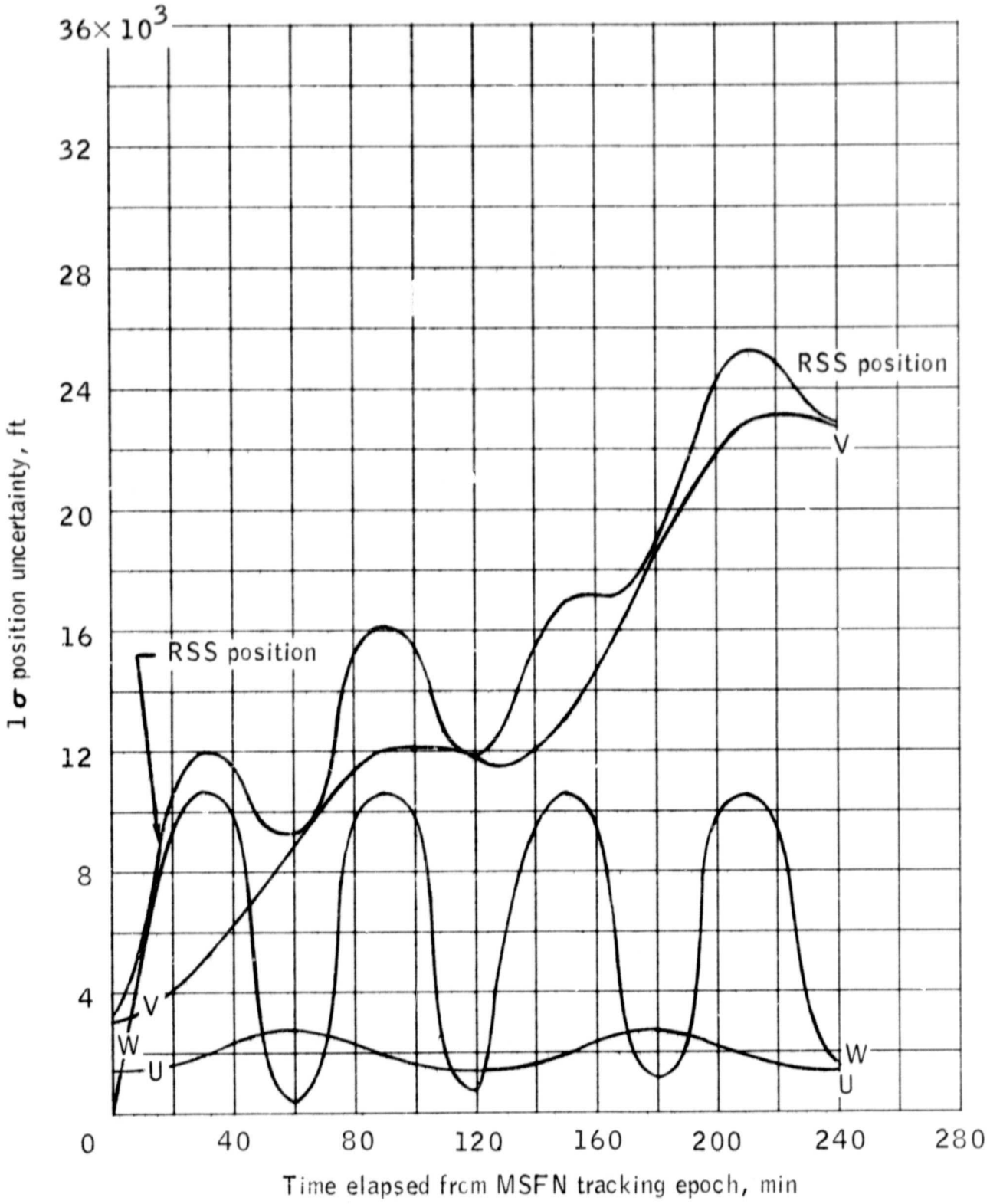

(a) One sigma position.

Figure 2.- One pass MSFN solution accuracies, Boeing R-2 lunar potential model.

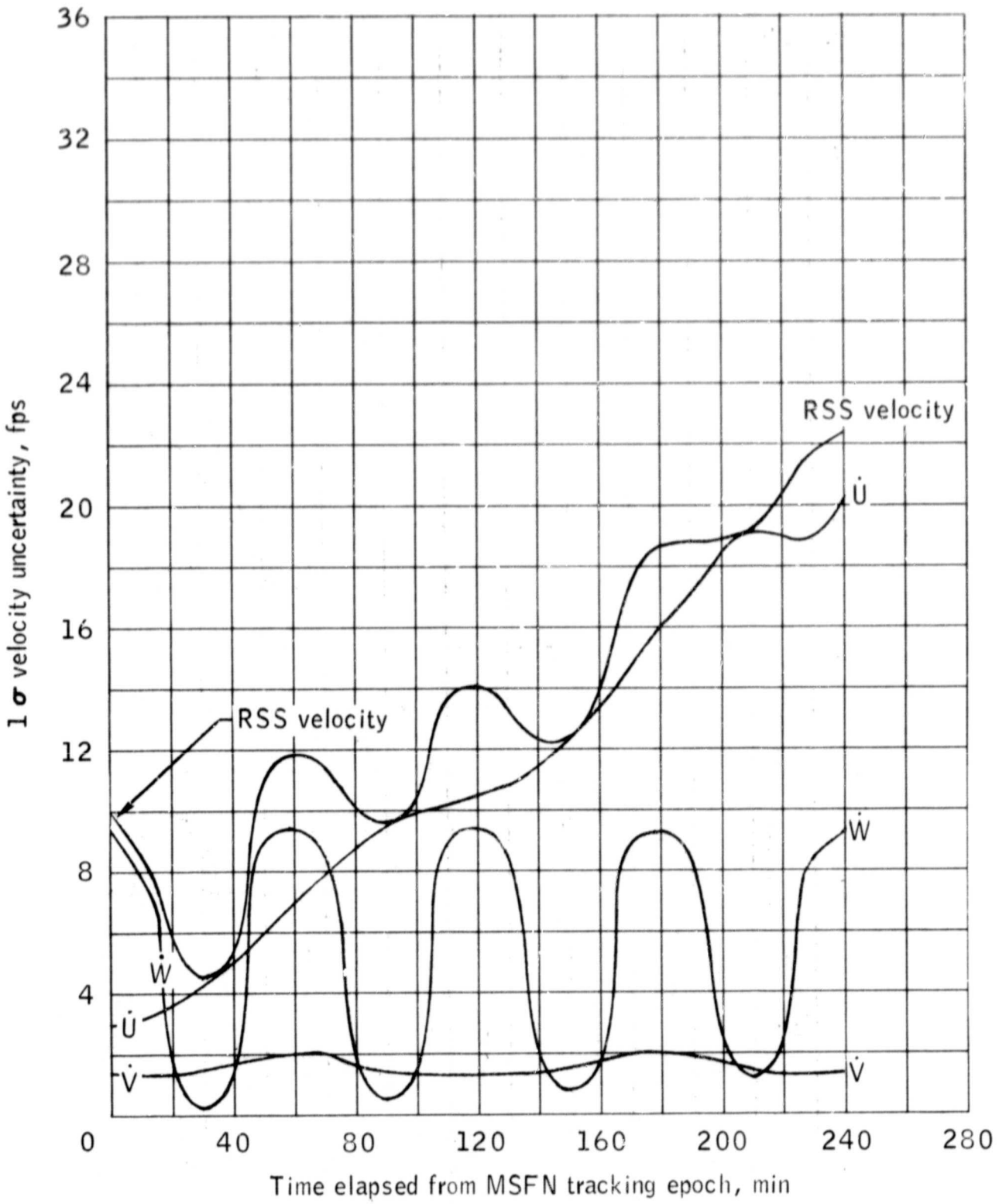

(b) One sigma velocity.

Figure 2.- Concluded.

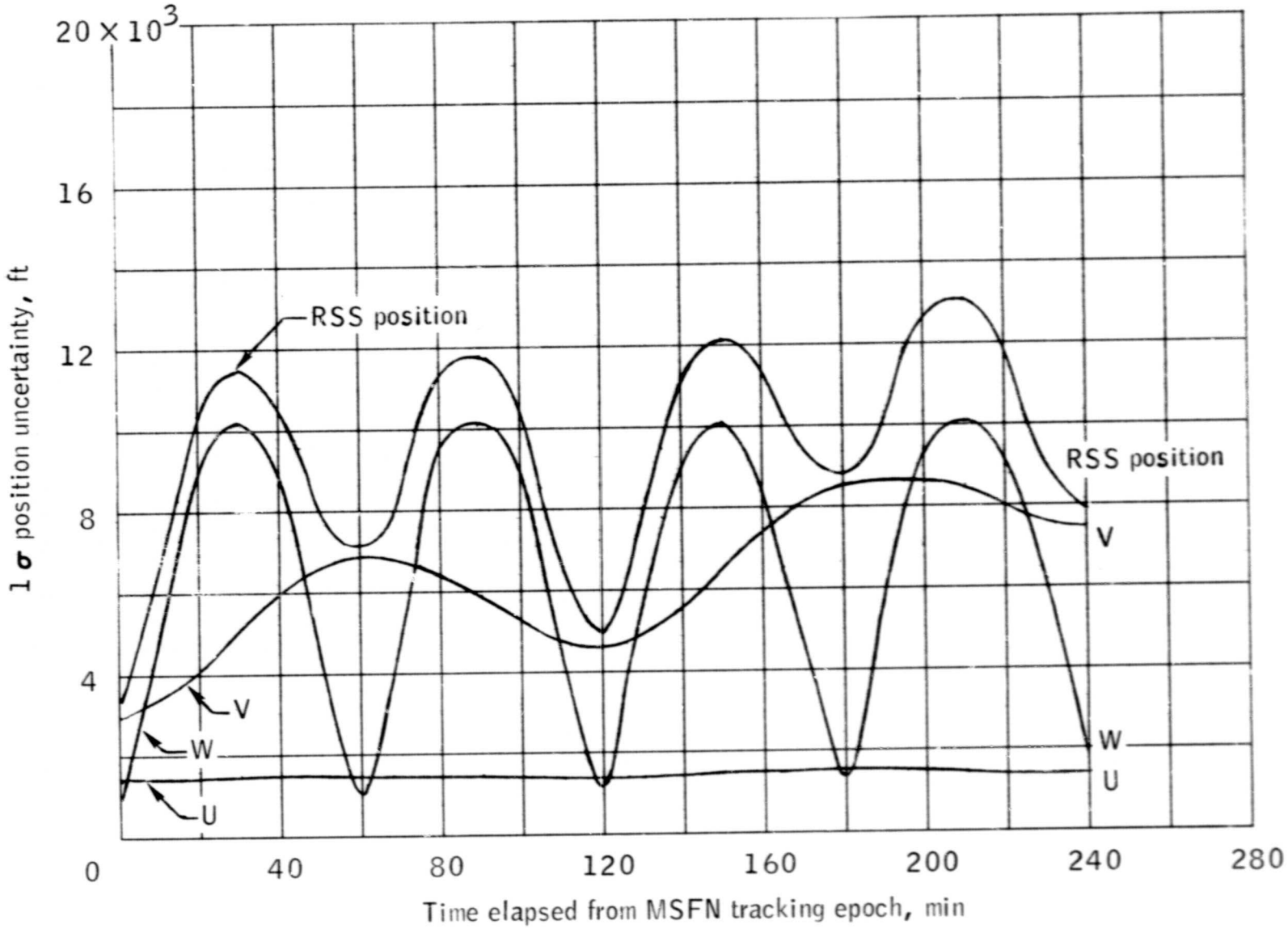

(a) One sigma position.

Figure 3.- Two pass MSFN solution accuracies, Boeing R-2 lunar potential model with out-of-plane solution constrained to one pass R-2 solution.

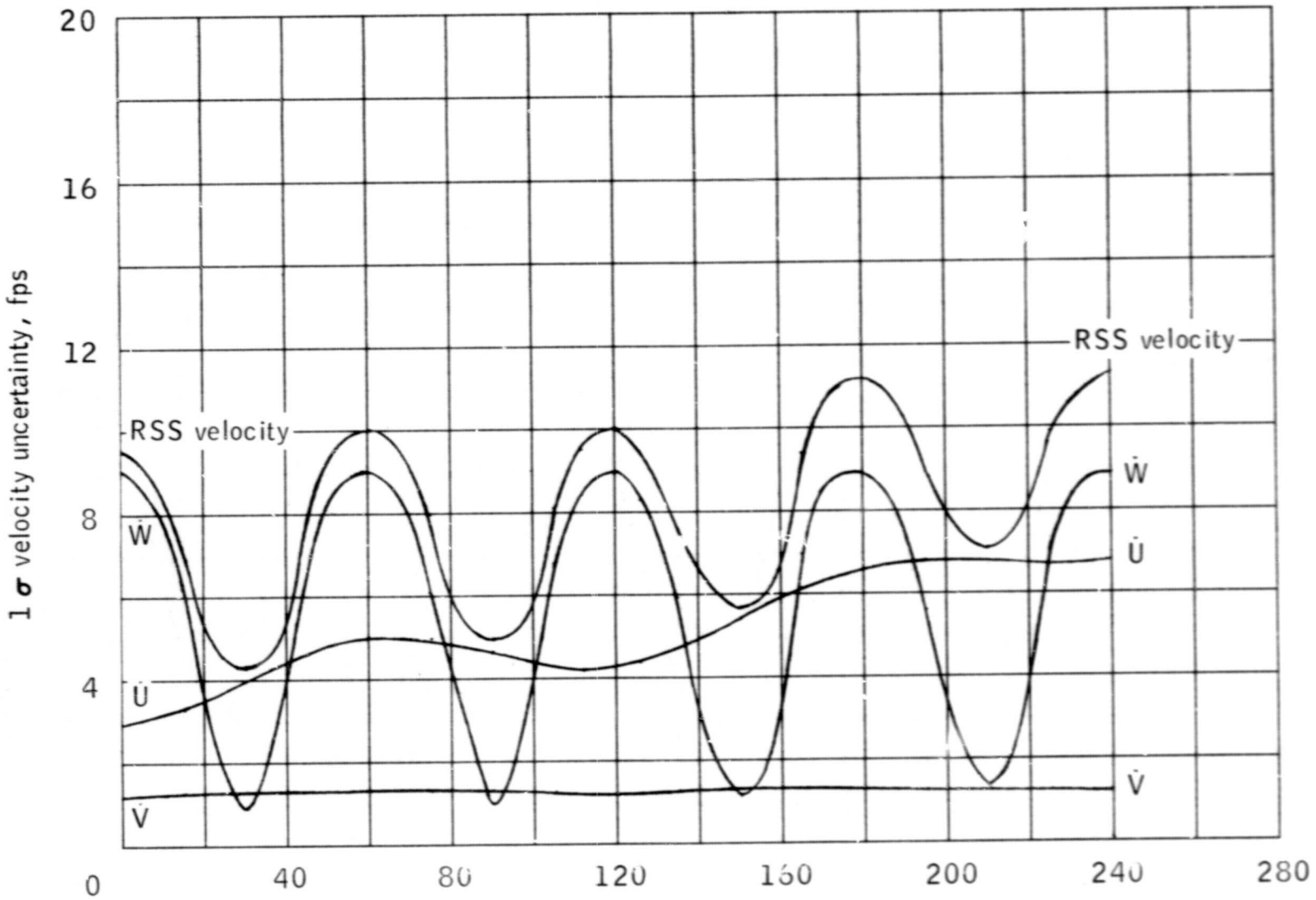

(b) One sigma velocity.

Figure 3.- Concluded.

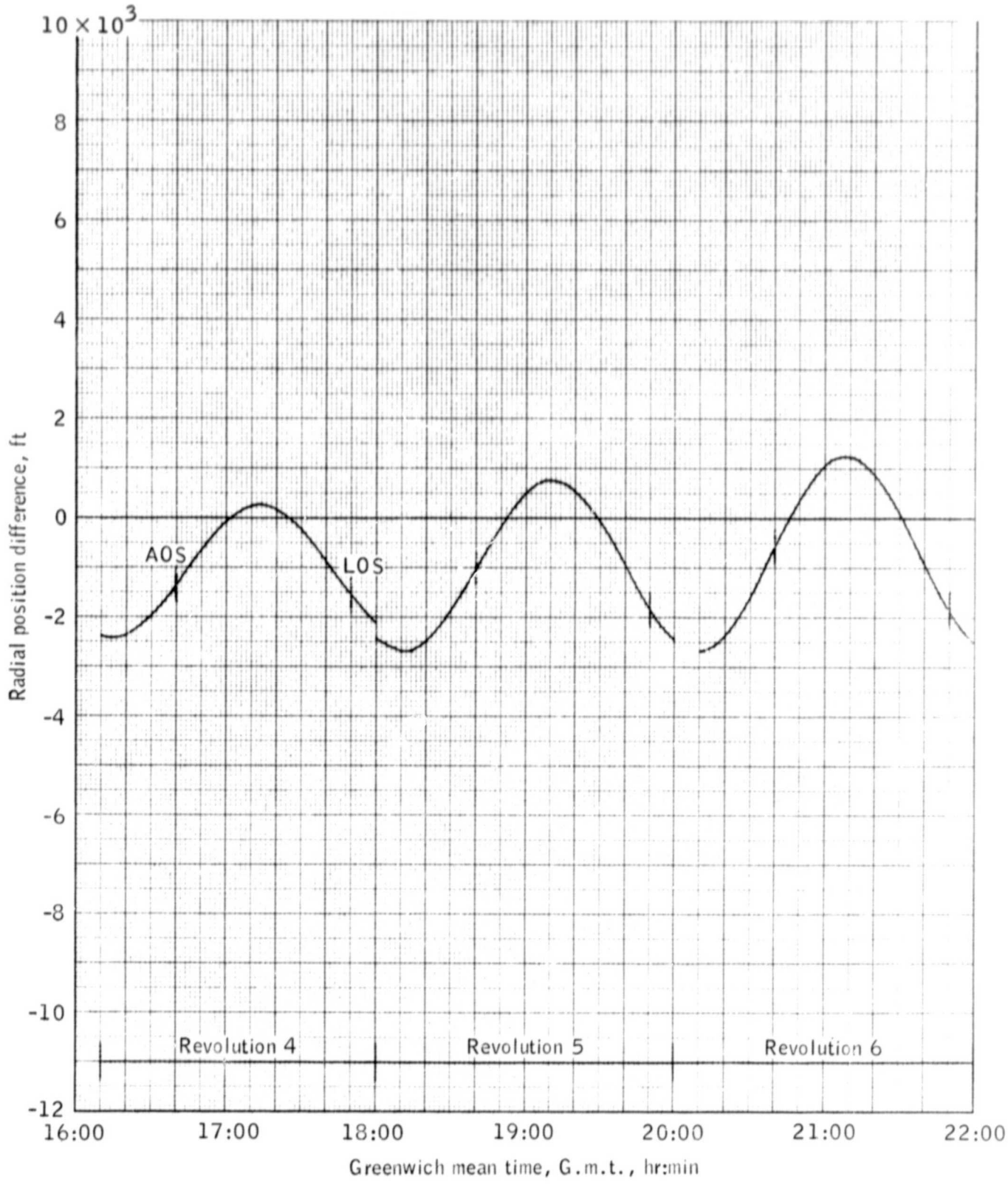

(a) Radial position difference.

Figure 4.- Apollo 8 state vector from revolutions 3 and 4, constrained fit compared with local one revolution unconstrained fits.

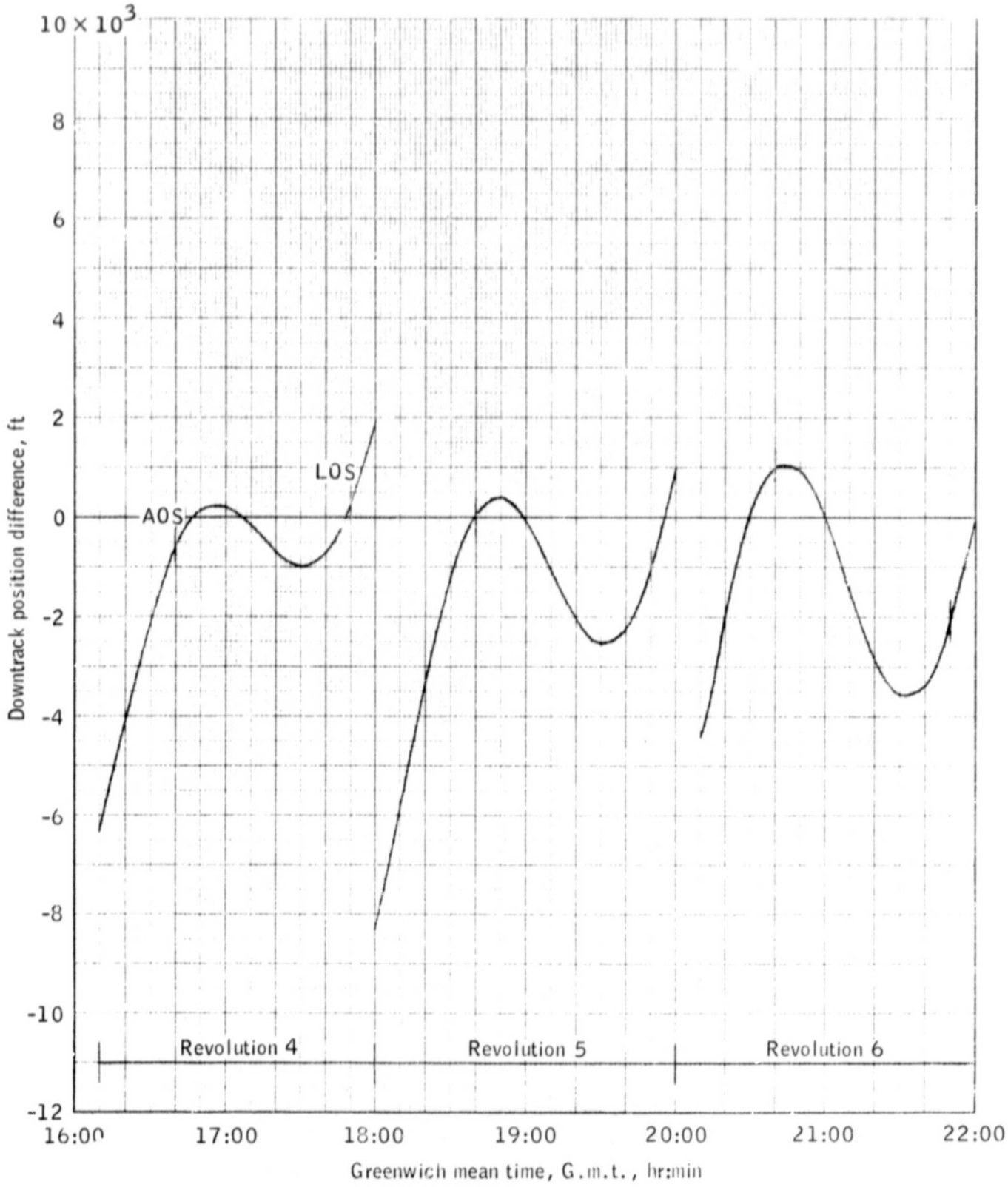

(b) Downtrack position difference.

Figure 4.- Continued.

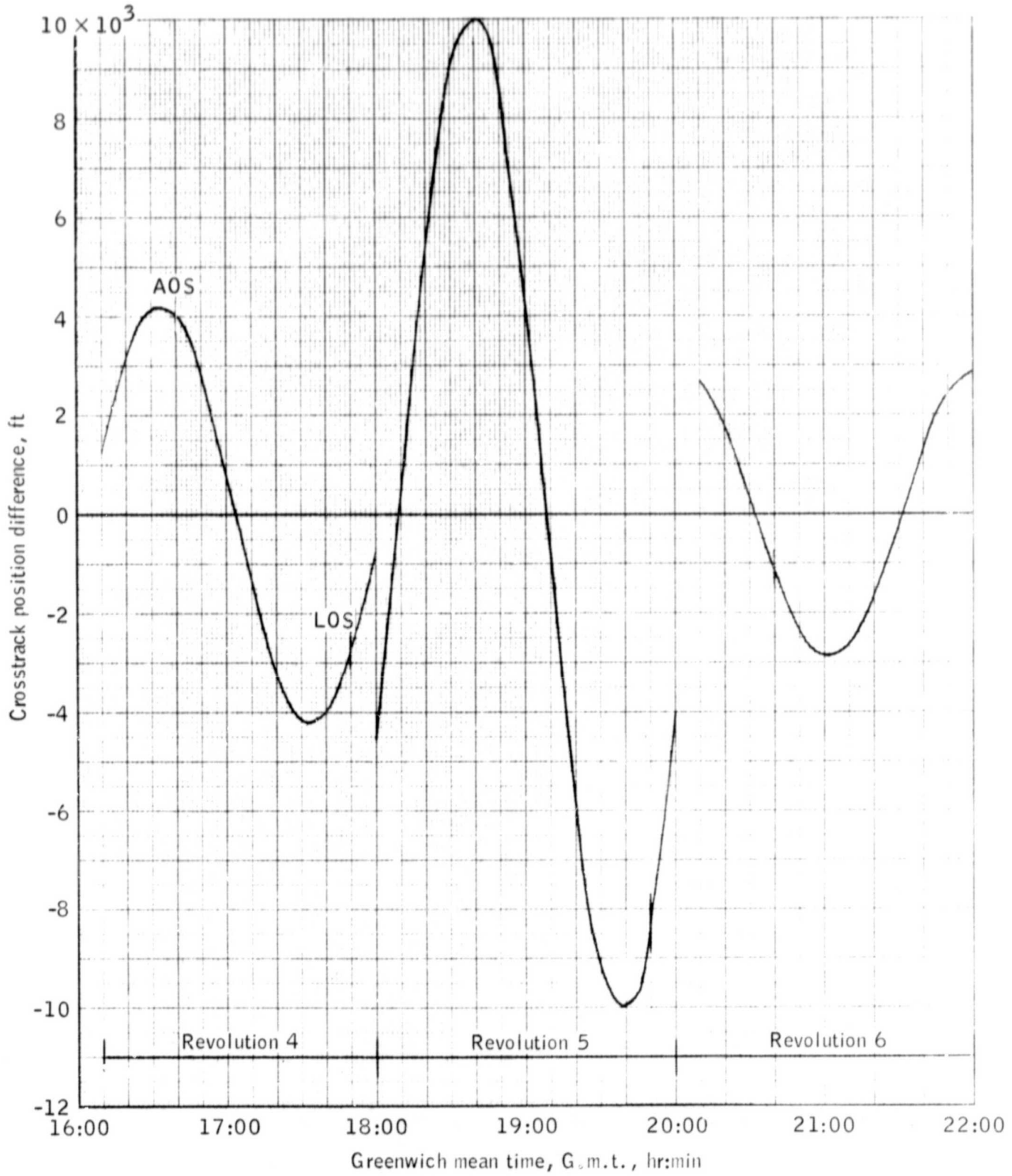

(c) Crosstrack position difference.

Figure 4.- Continued.

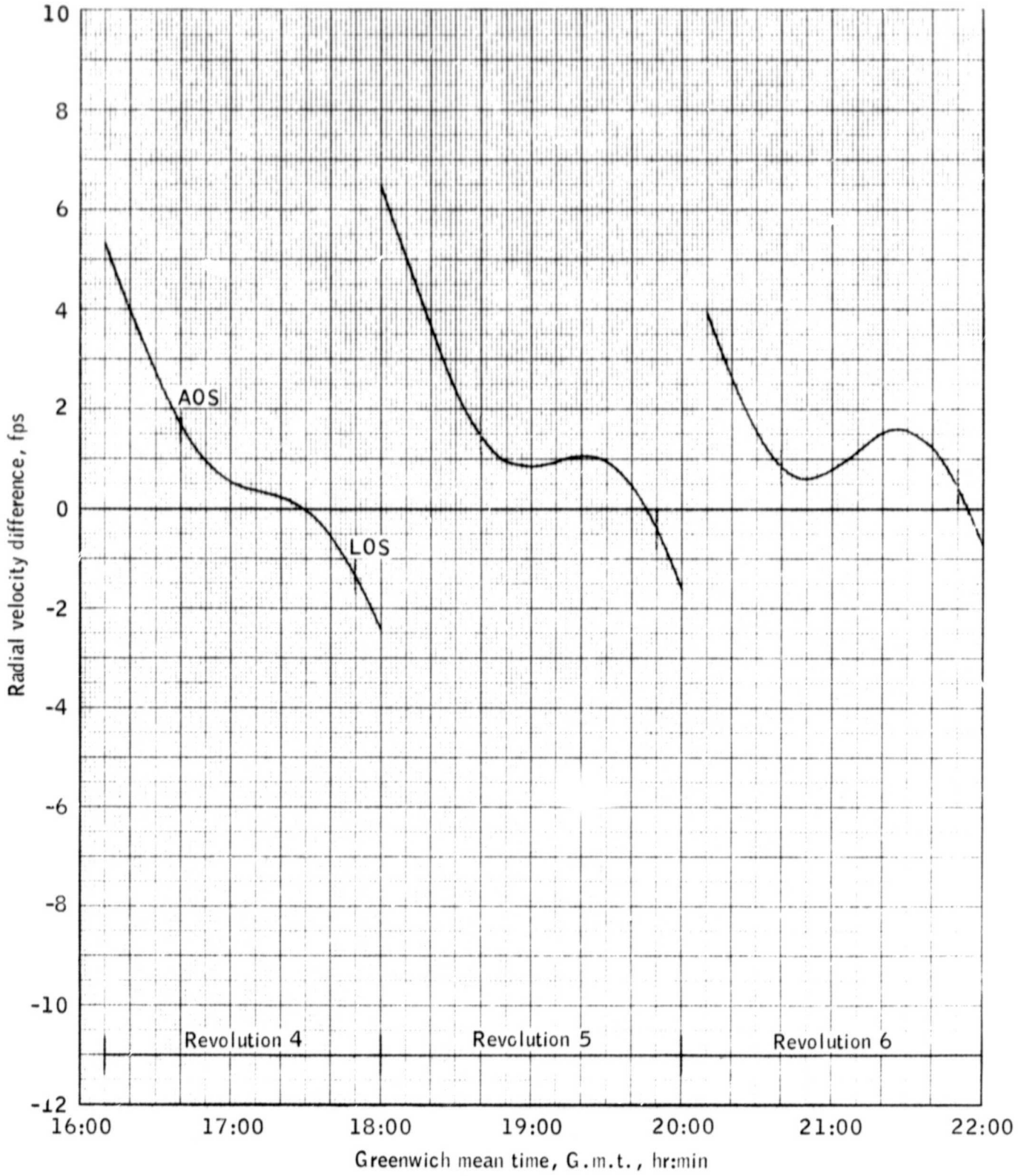

(d) Radial velocity difference.

Figure 4.- Continued.

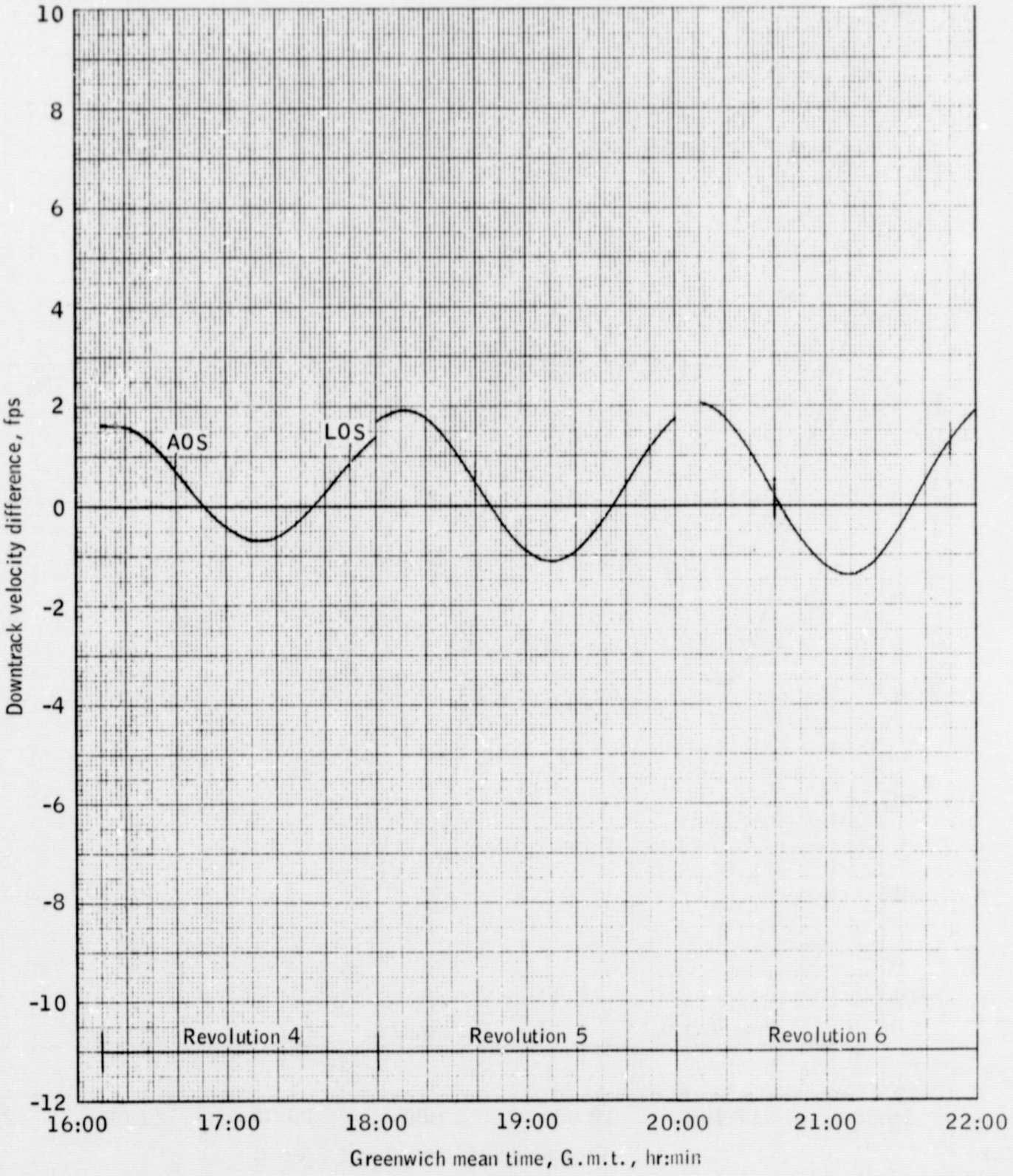

(e) Downtrack velocity difference.

Figure 4.- Continued.

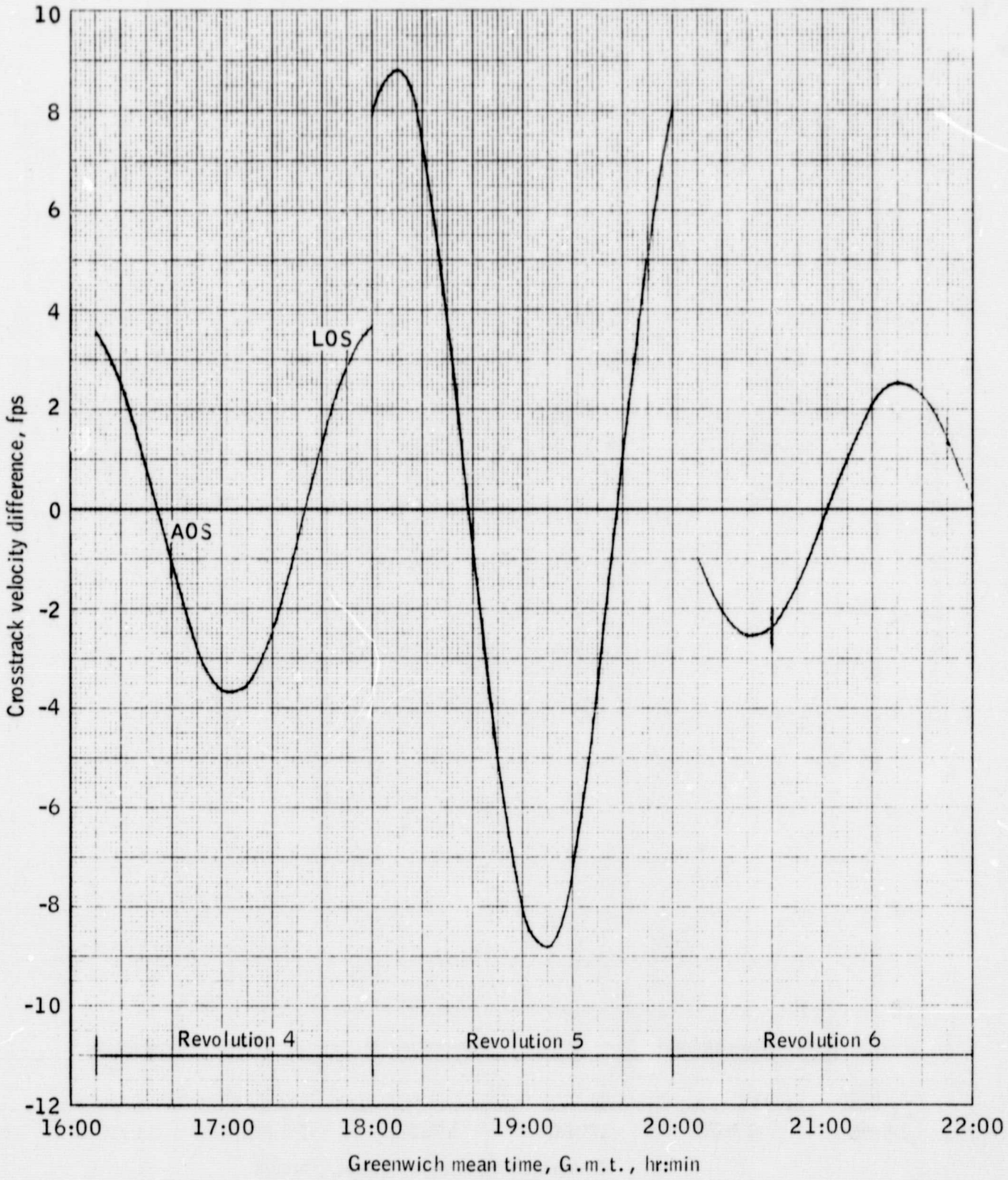

(f) Crosstrack velocity difference.

Figure 4.- Concluded.

APPENDIX

DERIVATION OF THE EQUATIONS FOR THE ERRORS IN RADIAL AND DOWN-TRACK VELOCITY AND THEIR COVARIANCES WITH RADIAL AND DOWN-TRACK POSITION ERRORS

APPENDIX

DERIVATION OF THE EQUATIONS FOR THE ERRORS IN RADIAL AND DOWN-TRACK VELOCITY AND THEIR COVARIANCES WITH RADIAL AND DOWN-TRACK POSITION ERRORS

RADIAL VELOCITY

The radial velocity error is assumed to be a function of flight-path angle error and phasing (i.e., down-track position) errors. Assuming that these two error sources are independent, one may write

$$\sigma_{\dot{u}}^2 = \left(\frac{\partial \dot{u}}{\partial v}\right)^2 \sigma_v^2 + \left(\frac{\partial \dot{u}}{\partial \gamma}\right)^2 \sigma_\gamma^2 \qquad \text{(A1)}$$

The equation relating radial velocity to flight-path angle is

$$\dot{u} = s \sin \gamma$$

so that $\frac{\partial \dot{u}}{\partial \gamma} = s \cos \gamma$. Since we are dealing with near-circular orbits, we may write

$$\begin{aligned} \gamma &\simeq 0 \\ \cos \gamma &\simeq 1 \qquad \text{(A2)} \\ \frac{\partial \dot{u}}{\partial \gamma} &\simeq s \end{aligned}$$

For circular orbits, in which the flight-path angle is constant, a phasing error translates into an error in the direction of the velocity vector, of the same magnitude. Thus an angular phasing error ϕ translates into a radial velocity error

$$\Delta\dot{u} = -s \sin \phi$$

where

$$\sin \phi \simeq \frac{\Delta v}{r}$$

So

$$\Delta\dot{u} = \frac{-s}{r} \Delta v$$

or

$$\frac{\partial \dot{u}}{\partial v} = - \frac{s}{r} \qquad \text{(A3)}$$

Substituting equations (A2) and (A3) into (A1) we have

$$\sigma_{\dot{u}}^2 = \left(- \frac{s}{r}\right)^2 \sigma_v^2 + s^2 \sigma_\gamma^2 \qquad \text{(A4)}$$

DOWN-TRACK VELOCITY

The down-track velocity error is also assumed to be caused by independent error sources. The first of these is the relationship between speed and radius derived from the energy equation assuming a fixed semimajor axis. The second is a period error. The period error translates directly into an error in semimajor axis and the energy equation is used to relate this error to speed. This results in the following equation

$$\sigma_{\dot{v}}^2 = \left(\frac{\partial \dot{v}}{\partial u}\right)^2 \sigma_u^2 + \left(\frac{\partial \dot{v}}{\partial a}\right)^2 \left(\frac{\partial a}{\partial \tau}\right)^2 \sigma_\tau^2 \qquad \text{(A5)}$$

Taking the partial derivatives of the energy equation for elliptical orbits

$$\frac{1}{a} = \frac{2}{r} - \frac{s^2}{\mu}$$

We have

$$\frac{\partial s}{\partial a} = \frac{\mu}{2sa^2}$$

and

$$\frac{\partial s}{\partial r} = \frac{-\mu}{r^2 s} \qquad \text{(A6)}$$

The relationship between period and semimajor axis is obtained from

$$\tau = 2\,\Pi\sqrt{\frac{a^3}{\mu}}$$

which can be solved for semimajor axis

$$a = \left(\frac{\mu^{1/2}\,\tau}{2\pi}\right)^{2/3}$$

which differentiates to yield

$$\frac{\partial a}{\partial \tau} = \frac{2a}{3\tau} \qquad \text{(A7)}$$

For nearly circular orbits the following relationships hold

$$u = r \text{ and } \dot{v} \simeq s$$

and from the energy equation

$$a \simeq r \text{ and } \mu \simeq rv^2. \qquad \text{(A8)}$$

An additional assumption involved in this derivation is that the down-track position error growth rate is a result of the period error which is contained entirely in the down-track velocity error at the tracking epoch. This assumption can be stated as

$$\sigma_\tau = \frac{v_g}{s} \tag{A9}$$

Substituting the relationships (A8) into equations (A6) and (A7), and substituting this result along with (A9) into equation (A5) we have

$$\sigma_{\dot{v}}^2 = \left(-\frac{s}{r}\right)^2 \sigma_u^2 + \left(\frac{v_g}{3\tau}\right)^2 \tag{A10}$$

COVARIANCES

Since the uncertainties in the in-plane velocity components were computed from the uncertainties in the in-plane position components, these errors are correlated. We may compute the correlation coefficients as follows

$$\sigma_{u\dot{v}} = \sigma_u\left(\frac{\partial \dot{v}}{\partial u}\sigma_u\right) = -\frac{s}{r}\sigma_u^2 \tag{A11}$$

$$\sigma_{v\dot{u}} = \sigma_v\left(\frac{\partial \dot{u}}{\partial v}\sigma_v\right) = -\frac{s}{r}\sigma_v^2$$

All other correlation coefficients are zero.

REFERENCES

1. Risdal, R. E.: Development of a Simple Lunar Model for Apollo - Final Report. Contract No. NAS 1-7954, The Boeing Co., Document No. D2-100819-1, December 20, 1968.

2. Proctor, Kenneth M.: Perturbed Trajectory Error Analysis Program, Computer Program Users' Manual. Contract NAS 9-5384, Project No. 1272, Program C032. Lockheed Electronics Co., Houston, Texas.